Available online at www.sciencedirect.com
ScienceDirect
Earth and Planetary Science Letters 259 (2007) 119–133
EPSL
www.elsevier.com/locate/epsl

Partial melting and melt percolation in the mantle: The message from Fe isotopes

Stefan Weyer [a,*], Dmitri A. Ionov [a,b]

[a] *Institute für Geowissenschaften, J.W. Goethe-Universität, Senckenberganlage 28, 60054 Frankfurt, Germany*
[b] *LTL, UMR-CNRS 6524, Département de Géologie, Université J. Monnet, 23 rue P. Michelon, 42023 Saint Etienne, France*

Received 9 October 2006; received in revised form 18 April 2007; accepted 23 April 2007
Available online 27 April 2007
Editor: R.W. Carlson

Abstract

High precision Fe isotope measurements have been performed on various mantle peridotites (fertile lherzolites, harzburgites, metasomatised Fe-enriched peridotites) and volcanic rocks (mainly oceanic basalts) from different localities and tectonic settings. The peridotites yield an average $\delta^{56}Fe = 0.01‰$ and are significantly lighter than the basalts (average $\delta^{56}Fe = 0.11‰$). Furthermore, the peridotites display a negative correlation of $\delta^{56}Fe$ with Mg# indicating a link between $\delta^{56}Fe$ and degrees of melt extraction. Taken together, these findings imply that Fe isotopes fractionate during partial melting, with heavy isotopes preferentially entering the melt.

The slope of depletion trends ($\delta^{56}Fe$ versus Mg#) of the peridotites was used to model Fe isotope fractionation during partial melting, resulting in $\alpha_{mantle\text{-}melt} \approx 1.0001–1.0003$ or $\ln\alpha_{mantle\text{-}melt} \approx 0.1–0.3‰$. In contrast to most other peridotites investigated in this study, spinel lherzolites and harzburgites from three localities (Horoman, Kamchatka and Lherz) are virtually unaffected by metasomatism. These three sites display a particularly good correlation and define an isotope fractionation factor of $\ln\alpha_{mantle\text{-}melt} \approx 0.3‰$. This modelled value implies Fe isotope fractionation between residual mantle and mantle-derived melts corresponding to $\Delta^{56}Fe_{mantle–basalt} \approx 0.2–0.3‰$, i.e. significantly higher than the observed difference between averages for all the peridotites and the basalts in this study (corresponding to $\Delta^{56}Fe_{mantle–basalt} \approx 0.1‰$). Either disequilibrium melting increased the modelled $\alpha_{mantle\text{-}melt}$ for these particular sites or the difference between average peridotite and basalt may be reduced by partial re-equilibration between the isotopically heavy basalts and the isotopically light depleted lithospheric mantle during melt ascent. The slope of the weaker $\delta^{56}Fe$–Mg# trend defined by the combined set of all mantle peridotites from this study is more consistent with the generally observed difference between peridotites and basalts; this slope was used here to estimate the Fe isotope composition of the fertile upper mantle (at Mg# = 0.894, $\delta^{56}Fe \approx 0.02 \pm 0.03‰$).

Besides partial melting, the Fe isotope composition of mantle peridotites can also be significantly modified by metasomatic events, e.g. melt percolation. At two localities (Tok, Siberia and Tariat, Mongolia) $\delta^{56}Fe$ correlates with iron contents of the peridotites, which was increased from about 8% to up to 14.5% FeO by post-melting melt percolation. This process produced a range of Fe isotope compositions in the percolation columns, from extremely light ($\delta^{56}Fe = -0.42‰$) to heavy ($\delta^{56}Fe = +0.17‰$). We propose reaction with isotopically heavy melts and diffusion (enrichment of light Fe isotopes) as the most likely processes that produced the large isotope variations at these sites. Thus, Fe isotopes might be used as a sensitive tracer to identify such metasomatic processes in the mantle.

Keywords: Fe isotopes; mantle; partial melting; diffusion; melt percolation; heavy stable isotopes; high temperature isotope fractionation

* Corresponding author.
E-mail address: stefan.weyer@em.uni-frankfurt.de (S. Weyer).

0012-821X/$ - see front matter © 2007 Published by Elsevier B.V.
doi:10.1016/j.epsl.2007.04.033

1. Introduction

Over its 4.5 billion years of history, the mantle has been modified by partial melting, crustal recycling and metasomatism. These events converted the original "primitive" mantle into heterogeneous mantle lithosphere with a complex pattern of depletion and refertilisation signatures. A major goal of mantle geochemistry is to characterize the processes responsible for the evolution of distinct mantle reservoirs and thus to improve our knowledge of mantle dynamics. Isotopic proxies (such as Sr, Nd, Hf, Pb or O) are frequently used to identify components of crustal recycling and to get information on time scales of mixing in the mantle (e.g. Hofmann et al., 2004 and references therein). In addition to that, stable isotopes, such as Fe and Li, may contribute to a better understanding of melting and transport processes and the role of oxygen fugacity and fluids during mantle metasomatism (Seitz et al., 2004, Williams et al., 2004, 2005; Elliott et al., 2006).

Iron is a major element in most common mantle minerals: olivine, orthopyroxene (opx), clinopyroxene (cpx), spinel, garnet, amphibole and mica. Recent studies revealed that Fe isotopes display a range of values in mantle rocks and their minerals (Zhu et al., 2001, 2002; Beard and Johnson, 2004; Weyer et al., 2004; Williams et al., 2004, 2005; Weyer et al., 2005; Schoenberg and von Blanckenburg, 2006). These studies reported variable Fe isotope fractionation between coexisting minerals of various mantle rocks, indicating isotopic disequilibrium and open system processes. Polyakov and Mineev (2000) used Mössbauer spectroscopy to determine β-factors (reduced isotopic partitioning function ratios) at $T=300$ K on the order of $10^3\ln\beta\approx 4$–8 for Fe^{2+} bearing minerals which are dominant in most common mantle rocks, and larger β-factors ($10^3\ln\beta\approx 10$–20) for Fe^{3+} bearing minerals. Applying a relation of $\ln\beta\sim 1/T^2$, isotope fractionation factors α in the order of $\ln\alpha_{A\text{-}B}\approx\Delta_{A\text{-}B}\approx 0$–0.4‰ should be expected at relevant mantle temperatures (1100 K–1700 K) between mantle minerals (or bulk solid mantle) and a partial melt. Much of the reported isotope variations within the mantle fall into this range. However, kinetic isotope fractionation during open system processes does not necessarily follow a $1/T^2$ relationship (Schauble, 2004) and chromatographic processes might further increase isotope fractionation in the mantle.

Weyer et al. (2005) found small but systematic differences in Fe isotopic compositions between averages for peridotites and basalts, with the mantle rocks being slightly isotopically lighter. They concluded that Fe isotopes fractionate during partial melting. This interpretation agrees with findings of Williams et al. (2004, 2005), who observed that Fe isotope compositions of minerals in variably depleted mantle rocks correlate with degrees of melt extraction. However, the magnitude of Fe isotope variations observed in these studies is difficult to explain by partial melting alone. This would imply a much stronger fractionation of Fe isotopes between mantle residues and melts than that observed by Weyer et al. (2005), which is unlikely from theoretical considerations. Williams et al. (2004, 2005) interpreted the high magnitude of Fe isotope variation in the mantle as a combined effect of metasomatic enrichment and partial melting.

The principal objective of this study is to provide better quantitative constraints on Fe isotope fractionation during mantle processes, such as partial melting and metasomatism, based on analyses of appropriate mantle rocks from various tectonic settings. We further aim to test Fe isotopes as a potential tracer to characterize mantle processes. We also provide new Fe isotope data on mantle-derived volcanic rocks (mainly MORB and OIB) from different localities to better characterize Fe isotope fractionation between the residual mantle and its primary melting products.

2. Sample selection

Mantle rocks from several localities were investigated in this study. They were chosen to represent (1) residues of different degrees of melt extraction from fertile mantle, and (2) products of post-melting metasomatic enrichment. These peridotites include xenoliths in late Cenozoic alkali basalts from Tok on the SE Siberian craton (Ionov et al., 2005a,b, 2006a,b) and from off-craton sites in Mongolia (Press et al., 1986; Ionov et al., 1994, 1998), xenoliths from the active Avacha andesitic volcano in Kamchatka representing a subduction zone setting as well as orogenic peridotites from Horoman (Takazawa et al., 2000), Lherz (Ionov et al., 2005b, 2006b) and (one sample each) from Beni Bouchera (Woodland et al., 1992; Williams et al., 2005) and Balmuccia (Weyer et al., 2003). All mantle-derived volcanic rocks analysed in this study are from ocean island or mid-ocean-ridge settings.

Most of the orogenic peridotites as well as xenoliths from Kamchatka in this study are residual peridotites with no or only moderate metasomatism; their modal and major element compositions are mainly controlled by different degrees of melt extraction. The samples from the Horoman Peridotite complex (Hokkaido, Japan) include two spinel harzburgites, two spinel lherzolites and two plagioclase lherzolites. Using major and trace element compositions Takazawa et al. (2000) interpreted these rocks as residues of polybaric melting that began in the garnet stability field. The samples from the Lherz massif (Woodland et al., 1996) include two lherzolites and two

harzburgites. They display a broad range of Mg# (0.902–0.923) and a narrow range of oxygen fugacities (0.1–0.6 ΔlogfO_2(FMQ)). All six xenoliths from Kamchatka in this study are harzburgites, with Mg# ranging from 0.906 to 0.916 and Al_2O_3 from 0.5 to 0.8%.

By comparison, the majority of peridotite xenoliths from Siberia and Mongolia we analysed are strongly metasomatised and many are enriched in iron. The largest number of samples of this study is from the Tok lava field near the SE margin of the Siberian craton. Four of the Tok xenoliths belong to the lherzolite–harzburgite (LH) series which groups variably metasomatised melt extraction residues with FeO from 7.3 to 8.3% and Mg# from 0.891 to 0.919 (Ionov et al., 2005a). Eight other Tok samples belong to the lherzolite–wehrlite (LW) series which formed by reaction of refractory residual peridotites with evolved (Mg# 0.6–0.7), Fe-rich silicate melts at high melt/rock ratios; their FeO contents range from 8.0 to 14.4% and Mg# from 0.889 to 0.829 (Ionov et al., 2005a). Two types of metasomatic processes may have been responsible for the formation of the LW series rocks. The most common type (labelled here as E1) was probably associated with infiltration of a Ca-rich, silica-undersaturated melt, resulting in the replacement of opx by cpx and thus transformation of lherzolites and harzburgites into wehrlites (Ionov et al., 2005a). Another type of enrichment (E2) produced high Fe concentrations without significant precipitation of metasomatic cpx (sample 10–11 with 14.4% FeO and Mg# 0.829). Thus, the E1 metasomatism is characterized by melt–rock reactions leading to large-scale phase transformations and modal changes. By contrast, the E2-type of metasomatism brings about Fe-enrichments through chemical exchange between the host peridotite and percolating Fe-rich melt without significant phase reactions. Four out of seven xenoliths from Tariat, central Mongolia in this study appear to have been affected by the E2-type process; their FeO contents range from 8.8 to 13.1% (Ionov et al., 1994, 1998). Another three Tariat xenoliths include fertile lherzolite Mo-101 (Press et al., 1986; Ionov and Hofmann, 2006) and two harzburgites (FeO 7.3–7.6%, Mg# 0.915–0.919, Ionov and Hofmann, 2006; Ionov, in press). A single harzburgite is from the Dariganga lava field in SE Mongolia (Ionov et al., 1994).

Nine out of ten partial melting products analysed in this study have basaltic compositions, one is dacite. Six of them were collected in mid-ocean ridges (East Pacific Rise, Kolbeinsey and the Knipovich Ridge; e.g. Haase, 2002) and four are from ocean islands (Azores, Reunion, Foundation and the Easter Island; e.g. Haase, 2002; Fretdorff and Haase, 2002). We analysed fresh basaltic to dacitic glasses extracted from these volcanic rocks. In addition, data on five basaltic and two peridotite reference samples from a previous publication (Weyer et al., 2005) are used here for modelling.

3. Analytical techniques

About 10–50 mg of either bulk rock powder or glass fragments was digested using a mixture of 2 ml HF and 1 ml HNO_3 in 7 ml Savilex® beakers on a hot plate. Purification of Fe was performed using a standard anion resin chromatographic procedure (Arnold et al., 2004; Weyer et al., 20005). Prior to measurements, the samples were diluted to 5 ppm Fe; 3 ppm of Cu standard NIST976 (internal mass bias monitor) was added to each diluted sample.

Isotope measurements were performed on a Finnigan-Neptune MC-ICP-MS instrument operated in high mass resolution mode (Weyer and Schwieters, 2003). In this mode, the mass resolution on all collectors is sufficient to completely eliminate all polyatomic mass interferences (e.g. $^{40}Ar^{14}N$ on ^{54}Fe, $^{40}Ar^{16}O$ on ^{56}Fe or $^{40}Ar^{16}OH$ on ^{57}Fe) and to produce flat-top peak sections ($\geq 10^{-4}$ ΔM/M) that are necessary for high precision measurements (Weyer and Schwieters, 2003; Arnold et al., 2004; Schoenberg and von Blankenburg, 2005; Weyer et al., 2005). A tandem quartz glass spray chamber (Finnigan SIS) combined with an ESI teflon microflow (50 µl) nebuliser was used for sample introduction. All Faraday collectors were equipped with 10^{11} Ω resistors. With this setup, a 20–25 V (2–$2.5 * 10^{-10}$ A) signal was usually achieved for a 5 ppm Fe solution (on ^{56}Fe). Instrumental mass bias was corrected assuming $^{65}Cu/^{63}Cu = 0.44563$ and applying the exponential law (Russell et al., 1978). Fe isotope standard IRMM-014 was measured between each sample. Fe isotope compositions are reported as $\delta(^{56}Fe/^{54}Fe)$ (further referred to as $\delta^{56}Fe$) relative to IRMM-014. ^{57}Fe was measured as well, and $\delta(^{57}Fe/^{54}Fe)$ (referred to as $\delta^{57}Fe$) was used for quality control and to monitor mass independent analytical artefacts. The delta values were calculated using the Cu mass bias corrected Fe isotope ratios and relative to the mean of the adjacent IRMM-014 standards. With this technique, combining sample-standard bracketing and the Cu mass bias correction, a precision of typically 0.03–0.06‰ (2 SD) for $\delta^{56}Fe$ (and 0.04–0.1‰ for $\delta^{57}Fe$) was routinely achieved for replicate measurements. Fe isotope analyses for all samples were replicated at least three times. Uncertainties generally correspond to 95% confidence intervals of averages of replicate analyses and were calculated using a "Student's *t*-distribution" (Weyer et al., 1978). The resulting uncertainties are about equal to "two standard deviations"

Table 1
Fe isotope compositions of bulk peridotites (and peridotite minerals)

Samples	Rock type/Mineral	cpx/opx	FeO	Mg#	δ^{56}Fe	Student's *t* (95% conf.)	*n*
SE Siberia (Tok)							
Lherzolite–harzburgite (LH) series							
2-9	Harzburgite	0.2	7.90	0.911	−0.051	0.034	4
6-0	Harzburgite	0.2	7.30	0.919	−0.005	0.026	3
6-1	Lherzolite	0.7	8.30	0.891	0.032	0.031	4
10-2	Harzburgite	0.3	7.60	0.915	0.000	0.045	3
Lherzolite–wehrlite (LW) series							
2-3	Low-opx lherz	2.3	8.90	0.880	0.028	0.031	3
2-10	Low-opx lherz	1.7	8.00	0.877	0.064	0.049	3
3-2 a)	Low-opx lherz	2.6	8.70	0.889	0.062	0.030	5
3-2 b)	Low-opx lherz				0.044	0.025	3
3-22 a)	Wehrlite	31.6	10.13	0.859	0.166	0.033	4
3-22 b)	Wehrlite				0.147	0.058	3
3-22-ol	Olivine				0.124	0.046	4
3-22-cpx	Cpx				0.162	0.041	5
8-10	Wehrlite	15.1	9.90	0.879	0.100	0.034	3
8-10-ol	Olivine				0.056	0.025	3
8-10-cpx	Cpx				0.058	0.025	3
10-1	Wehrlite	7.7	11.80	0.849	0.056	0.014	3
10-3	Wehrlite	78.0	13.12	0.839	0.058	0.043	4
10-11 a)	Lherzolite	0.6	14.38	0.829	−0.421	0.014	7
10-11 b)	Lherzolite				−0.428	0.042	3
10-11-ol	Olivine				−0.461	0.037	4
10-11-cpx	Cpx				−0.428	0.052	4
Mongolia							
Mo-101	Lherzolite	0.8	8.04	0.892	0.019	0.023	3
4500-18	Harzburgite	0.1	7.28	0.919	−0.031	0.066	3
4500-19d	Harzburgite	nd	7.60	0.915	−0.003	0.022	3
8530-24	Fe-rich harzburgite	nd	8.85	0.898	−0.033	0.040	3
8531-40	Fe-rich harzburgite	nd	8.80	0.900	−0.032	0.028	3
Z-9	Fe-rich lherzolite	0.3	9.32	0.886	−0.270	0.024	3
Hr-25	Fe-rich lherzolite	0.5	13.10	0.828	−0.326	0.021	3
BN-8	Harzburgite	0.1	7.13	0.919	−0.054	0.028	3
Horoman							
BZ-116	Harzburgite	nd	7.77	0.914	−0.011	0.032	4
BZ-216	Harzburgite	nd	7.60	0.915	−0.024	0.046	4
BZ-120	Lherzolite	nd	7.89	0.906	0.040	0.025	4
BZ-145	Lherzolite	nd	7.95	0.904	0.031	0.060	4
BZ-250	Plag-Lherzolite	nd	7.68	0.904	0.087	0.044	4
BZ-255	Plag-Lherzolite	nd	8.02	0.898	−0.045	0.027	4
Kamchatka							
Av-1	Harzburgite	<0.1	8.13	0.909	−0.015	0.045	4
Av-4	Harzburgite	<0.1	8.07	0.906	−0.001	0.040	4
Av-6	Harzburgite	<0.1	8.24	0.909	−0.017	0.020	4
Av-8	Harzburgite	<0.1	7.74	0.911	−0.005	0.013	4
Av-16	Harzburgite	<0.1	7.55	0.916	−0.064	0.027	4
Av17	Harzburgite	<0.1	7.83	0.914	−0.028	0.005	4
Lherz							
Py35	Lherzolite	nd	nd	0.904[a]	0.021	0.026	3
Py18[b]	Lherzolite	nd	nd	0.906[a]	0.003	0.038	3
Py6	Harzburgite	nd	nd	0.916[a]	−0.049	0.044	3
Py11	Harzburgite	nd	nd	0.923[a]	−0.066	0.039	3

Table 1 (*continued*)

Samples	Rock type/Mineral	cpx/opx	FeO	Mg#	δ^{56}Fe	Student's *t* (95% conf.)	*n*
Balmuccia							
BM90-21[b]	Lherzolite	nd	8.74	0.896	0.008	0.041	7
Beni Bouchera							
5-209[b]	Lherzolite	nd	nd	0.909	0.041	0.050	3
JP-1[b]		nd	7.60	0.913	0.025	0.018	10
PCC-1[b]		nd	7.92	0.907	0.043	0.023	3
Whole rock mean					**−0.021**	**0.040**	**40**
Whole rock mean[c]					**0.014**	**0.018**	**37**
Mg# <0.885[c]					**0.081**	**0.051**	**6**
Mg# >0.905					**−0.013**	**0.015**	**21**

[a] Mg# of olivine.
[b] Data from Weyer et al. (2005).
[c] Except samples 10-11 (Tok) and Z9, HR25 (Mongolia) which where overprinted by E2-type of metasomatism (probably modified by Fe-diffusion).

for $n=3$ measurements, but lower for a higher number of replicates.

4. Results

Fe isotope composition was determined on 35 whole-rock peridotites, 3 hand-picked olivine and cpx separates and 10 fresh volcanic glasses. Delta ^{56}Fe of the whole-rock peridotites range from −0.42 to +0.16‰ while the basalts display a range of δ^{56}Fe from +0.05 to +0.24‰ (Tables 1 and 2, Fig. 1). Fe isotope composition of the olivine and cpx separates is identical to those of their bulk rocks within analytical uncertainties. Average δ^{56}Fe (−0.02‰) calculated for all the mantle rocks in this study is distinctly lower than average δ^{56}Fe of the basalts (+0.11‰). Even if one excludes three extremely isotopically light samples, which underwent E2-type metasomatism and appear to be very rare in the mantle

Table 2
Fe isotope compositions of partial melting products

Samples	Locality	Rock type	Mg#	δ^{56}Fe	Student's *t* (95% conf.)	*n*
BIR-1 a)	Iceland	Basalt	0.593	0.054	0.017	14
BIR-1 b)				0.057	0.020	8
SO62 218G a)	EPR	Basalt	0.653	0.142	0.029	6
SO62 218G b)				0.136	0.030	6
SO62 258G	EPR	Basalt	0.478	0.078	0.034	4
SO62 224G	EPR	Basalt	0.721	0.068	0.036	4
PL96-53	Knipovich Ridge	Basalt	0.551	0.176	0.014	8
666 DS-3	Kolbeinsey	Basalt	0.451	0.063	0.032	4
616 DS-2	Kolbeinsey	Basalt	0.470	0.059	0.027	4
17DS-2gl a)	Reunion	Basalt	0.361	0.176	0.038	6
17DS-2gl b)				0.181	0.028	7
37 DS-1 gl a)	Easter Island	Basalt	0.459	0.241	0.031	6
37 DS-1 gl b)				0.244	0.025	8
SM9701 a)	Azores	Basalt	0.422	0.135	0.034	6
SM9701 b)				0.149	0.019	6
SO157-65DS1 a)	Foundation	Dacite	0.217	0.127	0.023	6
SO157-65DS1 b)				0.145	0.040	4
BHVO-1	Hawaii	Basalt	0.506	0.117	0.028	3
BCR	Columia river	Basalt	0.469	0.079	0.047	3
JB-2	Oshima-volc	Basalt	0.358	0.056	0.030	3
KAL-1	Alexo, Ontario	Komatiite		0.071	0.022	4
Mean				**0.111**	**0.032**	
MORB mean				**0.091**	**0.042**	
OIB mean				**0.163**	**0.048**	

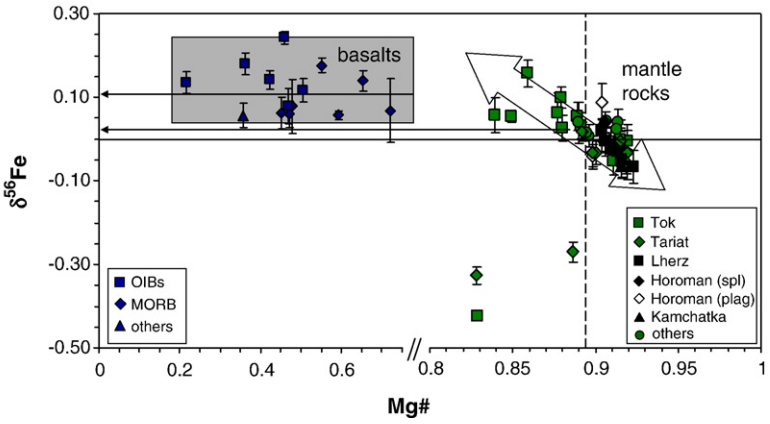

Fig. 1. Summary of Fe isotope compositions for all basalts and mantle peridotites of this study plotted versus Mg#. The majority of the peridotites define a broad negative correlation of δ^{56}Fe and Mg# (indicated with the block arrow), except for three samples. The latter are lherzolites, which are enriched in Fe (hence have low Mg#) and have extremely light Fe isotope compositions. δ^{56}Fe and Mg# are not correlated in the basalts. Thin arrows indicate average δ^{56}Fe for basalts and δ^{56}Fe of the fertile upper mantle at Mg#=0.894 (vertical dashed line, McDonough and Sun, 1995). δ^{56}Fe at Mg#=0.894 is modelled in Fig. 3a, using linear regression. Basalts are significantly isotopically heavier in average than the upper mantle.

(see Discussion), the average for the peridotites remains significantly lighter (with δ^{56}Fe=+0.01‰) than for the basalts. This difference implies fractionation of Fe isotopes during partial melting (Williams et al., 2005; Weyer et al., 2005; Schoenberg and von Blanckenburg, 2006; Weyer et al., in press). In the present study, we analysed mantle rocks, which cover a broad range of Mg# from fertile (Mg# 0.890) to highly depleted (Mg#=0.923) as well as variably Fe-enriched samples (Mg# down to 0.828; Fig. 1). With few exceptions, their Fe isotope compositions correlate with the degree of partial melting (or post-melting Fe-enrichment) as expressed by their Mg# (Williams et al., 2005). This latter finding supports the hypothesis that Fe isotopes fractionate during partial melting as inferred earlier from systematic Fe isotope differences between peridotites and basalts (Weyer et al., 2005; Schoenberg and von Blanckenburg, 2006; Weyer et al., in press; this study).

The majority of the Fe-enriched peridotites (Mg#< 0.89) tend to have heavier Fe isotope compositions relative to those of the melting residues. Some of the strongly metasomatised samples from Tok and Mongolia are particularly Fe-rich (11.8–14.4% FeO), with Mg# as low as 0.83. The majority of those peridotites (typically E1-type) follow the overall negative δ^{56}Fe–Mg# trend (Fig. 1). However, two Fe-rich peridotites from Tariat and one sample from Tok, all of them belonging to the E2 enrichment type, have particularly light Fe isotope compositions and do not follow the general trend in Fig. 1. The depleted harzburgites from Tok and Tariat, together with the peridotites that were affected by the E1 type metasomatism also show moderate to robust correlation (R^2=0.5–0.9) of Fe isotope composition with enrichments of cpx, CaO, FeO, Mg#, Zr (Fig. 2a–e) and other moderately incompatible elements, such as heavy REE (not shown). These samples display no or only poor correlations of Fe isotopes with highly incompatible elements, such as Ba (Fig. 2f) or LREE (not shown). Two of the E1-type samples (10-1 and 10-3) might have been additionally affected by E2-type metasomatism to some degree as indicated by their low δ^{56}Fe values (Fig. 2c+d). For that reason, these two samples are not taken into account for the calculation of regression lines in Fig. 2.

In contrast to the peridotites, the mantle-derived volcanic rocks show no systematic variation of Fe isotope compositions with Mg# (which for basalts mainly depends on the degree of olivine fractionation prior to eruption) or other chemical parameters (Fig. 1). However, OIBs appear to be isotopically heavier on average (δ^{56}Fe=0.163±0.048) than MORBs (δ^{56}Fe=0.091±0.042), although these values overlap within analytical uncertainties (at 95% confidence levels).

5. Discussion

5.1. Fe isotope fractionation during partial melting

The difference in average Fe isotope compositions of partial melting products (basalts) and residual mantle rocks, and correlation of δ^{56}Fe with indicators of depletion degrees in mantle rocks indicate that Fe isotopes fractionate during partial melting in the mantle (Williams et al., 2005; Weyer et al., 2005, in press). The effect of melt extraction on Fe isotope composition of the residue was modelled assuming variable isotope fractionation factors $\alpha_{\text{mantle-melt}}$ and using either pure batch or pure

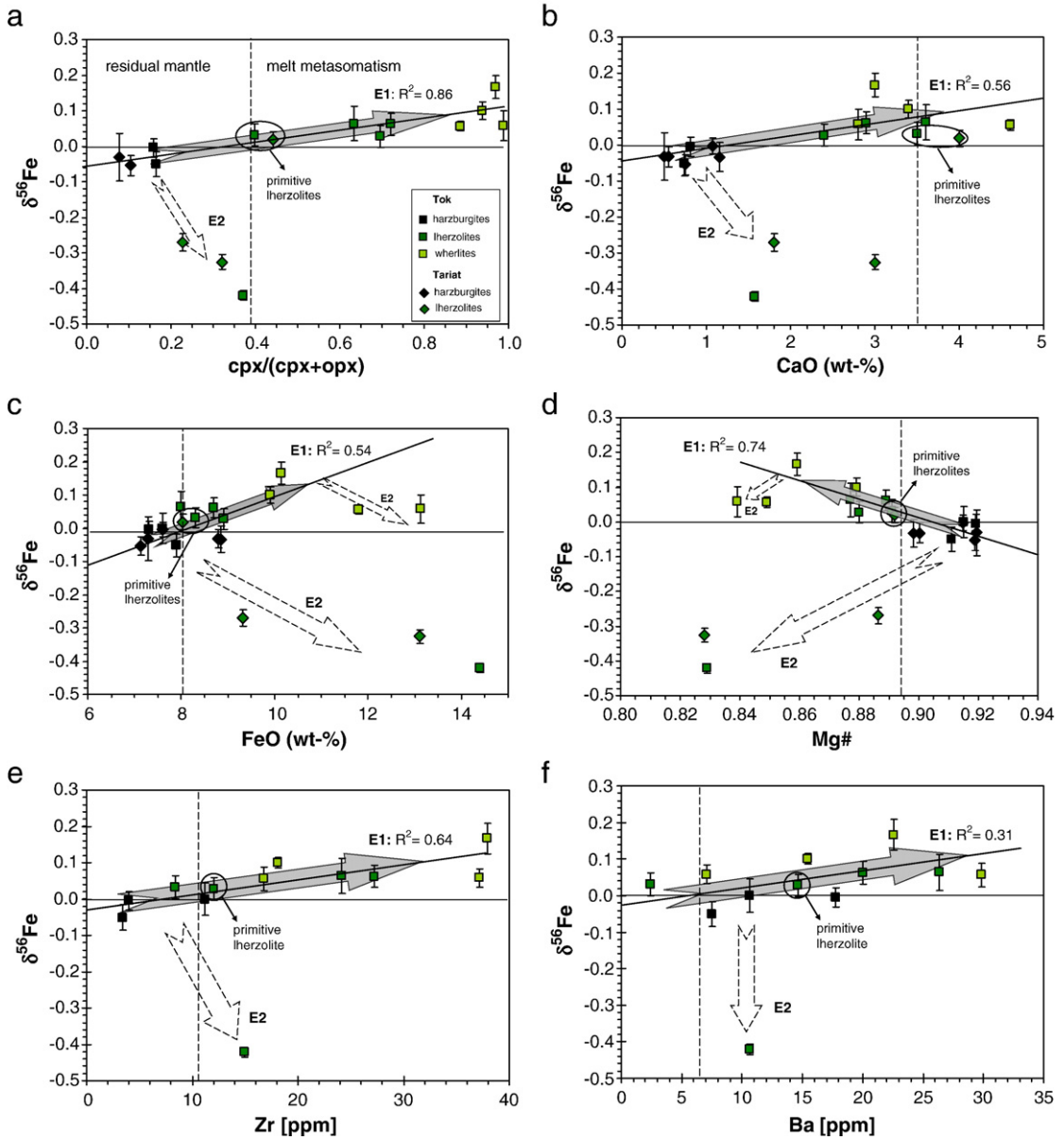

Fig. 2. Plot of δ^{56}Fe versus: (a) cpx/(cpx+opx), (b) CaO, (c) FeO, (d) Mg#, (e) Zr and (f) Ba for peridotites from Tok and Tariat. Two types of metasomatic enrichment (E1 and E2) resulting in different Fe isotope compositions can be distinguished for these localities. E1 is characterized by a positive correlation of δ^{56}Fe and cpx, CaO, FeO, Mg# and immobile trace elements, such as Zr (a–e). Highly incompatible and mobile elements are not or only weakly correlated with δ^{56}Fe (f). E2 is characterized by extremely light Fe isotope compositions, also combined with an increase in Fe (and a decrease in Mg#), but no significant increase in cpx, CaO, Zr and Ba. The thick solid line is calculated using linear regression for E1-type enriched samples (R^2 values are given for each regression). Samples 10-1 and 10-3 probably underwent E2-type, additionally to E1-type, enrichment and were thus excluded from calculations of the linear regression (see text for further discussion). Block arrows schematically indicating the direction of E1 and E2 enrichment. The dashed vertical line always represents the primitive mantle value (McDonough and Sun, 1995).

fractional melting models (similar to the modelling of Williams et al. (2005)). The objective of the model was to get an estimate for $\alpha_{\text{mantle-melt}}$ from the depletion trend observed in the mantle rocks and to prove whether this estimate agrees with the estimate we obtained from average δ^{56}Fe of mantle peridotites and partial melts above.

The relationship between the degree of partial melting F and the Mg# as well as the partition coefficient D_{Fe} during partial melting was estimated using the experimental data of Herzberg (2004). The relationship between F and D_{Fe} (or F and Mg#) varies with pressure (Langmuir et al., 1992; Walter, 1992; Kinzler, 1997;

Herzberg, 2004). For our modelling, which we intend to apply to a variety of mantle rocks with different partial melting histories, we used the data set which was determined at 2 GPa (Herzberg, 2004) and a constant partition coefficient of $D_{Fe}=0.9$. These parameters probably best match the conditions of melting events for the majority of the studied sample localities. Additionally, the partition coefficient is generally close to 1 and the Fe concentration does not change much during partial melting. Thus, the model is not very sensitive to exact values of D. Since inter-mineral partition coefficients for Fe isotopes are poorly constrained, but probably do not exceed 0.2‰ (Beard and Johnson, 2004; Williams et al., 2005; Weyer et al., in press), we did not apply non-modal melting models. The magnitude of modelled Fe isotope fractionation factors is not likely to be sensitive to modal versus non-modal melting because the Fe budget is mainly controlled by olivine and opx (Weyer et al., in press), which have very similar Fe isotope compositions and which are never exhausted during partial melting. A more detailed description of the modelling is provided in the Supplementary data.

If all mantle rocks from all localities in this study are considered in the modelling (Fig. 3a), the correlation of δ^{56}Fe and the Mg# (further referred as trend A) is very weak, i.e. $R^2 \approx 0.3$ of linear regression. The slope of the

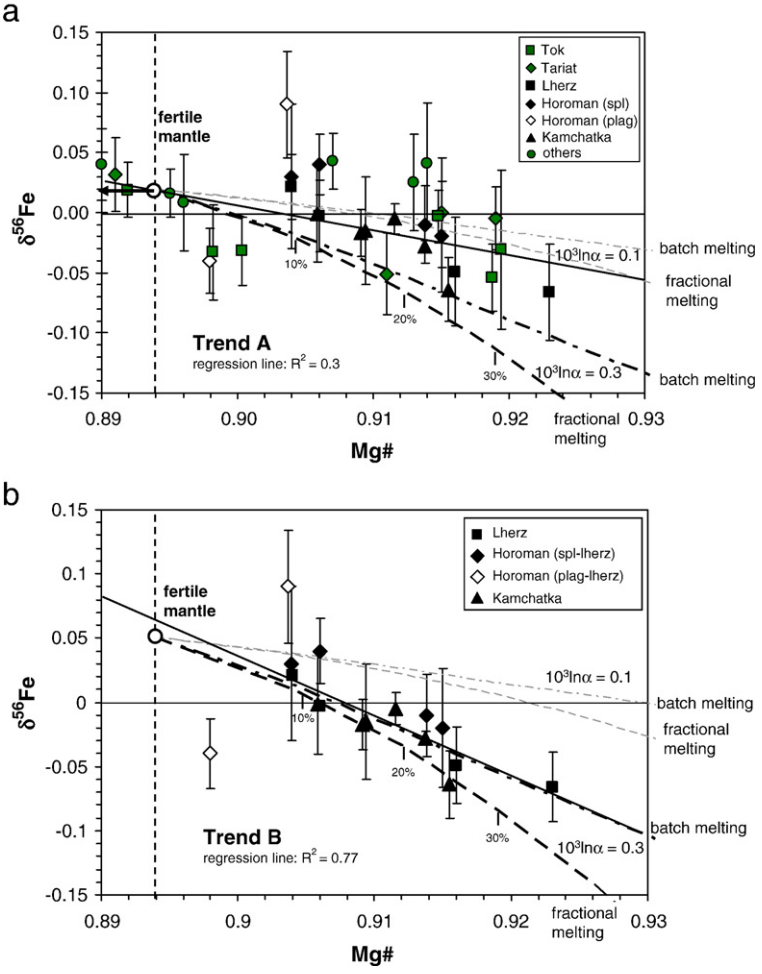

Fig. 3. Plot of δ^{56}Fe versus Mg# for fertile and depleted peridotites with Mg# >0.89. Included are modelled curves of Fe isotope fractionation during partial melting assuming different isotope fractionation factors α ($\ln\alpha \approx 0.1$‰: thin grey lines; $\ln\alpha = 0.3$‰: bold lines) and either pure batch (dashed line with dots) or fractional melting (dashed line); tick marks indicate degrees of melt extraction; see text and electronic supplement for details of modelling. Also shown are regression lines (solid). (a) Considering samples from all localities the correlation (trend A) is weak with best fit to $\ln\alpha \approx 0.1$‰. Trend A might give the best estimate for the Fe isotope composition of the fertile upper mantle, since samples from many different localities are included: at Mg#=0.894 (thin dashed vertical line), $\delta^{56}Fe \approx 0.02$. (b) Considering only spinel peridotites from Horoman, Kamchatka and Lherz, the correlation (trend B) is much better and the best fit is to $\ln\alpha = 0.3$‰ with a slightly higher initial of $\delta^{56}Fe \approx 0.05$. Trend B might give the best estimate for the fractionation factor α, since the original partial melting trend appears to be least disturbed.

regression line best agrees with Fe isotope fractionation during partial melting described by $\ln\alpha_{\text{mantle-melt}} \approx 0.1‰$. This isotope fractionation factor is consistent with the estimate derived from the difference in Fe isotope composition of average basalts and fertile mantle ($\Delta^{56}Fe_{\text{mantle-melt}} \approx 0.09$). The great majority of peridotites in this study come from five localities, with four or more samples representing each locality. Of those five sample suites, spinel lherzolites from three localities (Horoman, Kamchatka and Lherz) show no or only little evidence for post-melting enrichments. By contrast, the majority of samples from the other two sites (Tok and Tariat) in this study are strongly metasomatised. Trend B (Fig. 3b) considers only spinel lherzolites from Horoman, Kamchatka and Lherz. These virtually unmetasomatised sample suites define nearly identical regression lines with a much better correlation of δ^{56}Fewith Mg# ($R^2 = 0.77$), although their range in Mg# is rather small compare to the entire range defined by all depleted samples. Trend B can be modelled as Fe isotope fractionation during partial melting with $\ln\alpha_{\text{mantle-melt}} \approx 0.3‰$. Within the uncertainty of the model, batch melting cannot be distinguished from fractional melting, since the modelled trends only differ significantly at very high degrees of melting.

As noted above, the contents of major and moderately incompatible trace elements in spinel peridotites from these localities show a record of melt extraction and do not appear to be affected by metasomatism. Importantly, the contents of FeO in all the studied samples from Horoman, Kamchatka and Lherz are <8.1% (i.e. primitive mantle McDonough and Sun, 1995) and show no evidence for post-melting Fe-enrichments. Trace element patterns of the Kamchatka peridotites and the spinel peridotites from Horoman (Takazawa et al., 2000) indicate no or only minor enrichments in highly incompatible elements, e.g. they typically retain low LREE/HREE characteristic of melting residues. The harzburgites from Lherz show more significant enrichments in the highly incompatible elements and probably have a complex enrichment history (Bodinier et al., 2004). However, the metasomatic overprint of the Lherz harzburgites probably only affected the highly incompatible elements, but not the more compatible elements (such as Fe). The nearly identical correlations between δ^{56}Fe and Mg# obtained here for the Horoman, Kamchatka and Lherz peridotites indicate that these trends are most likely produced by partial melting. Thus, trend B should be more suitable to model Fe isotope fractionation during partial melting in the mantle than trend A.

Isotope fractionation with $\ln\alpha_{\text{mantle-melt}}$ on the order of 0.1–0.3‰, as indicated by the trends A and B, is more realistic than that derived in earlier work from other peridotite suites (Willimas et al., 2005). Theoretical modelling (Polyakov and Mineev, 2000) predicts that isotope fractionation at partial melting temperatures between Fe^{II} and Fe^{III} bearing minerals can easily exceed 0.3‰. By comparison, isotope fractionation between Fe^{II} bearing minerals is more limited. No theoretical data are available on Fe isotope fractionation between a basaltic melt and peridotites. Isotopically heavier melts may be produced if: (1) Fe^{III} is more incompatible than Fe^{II} during partial melting and (2) heavy iron isotopes favour Fe^{III} complexes. Such behaviour was initially predicted by theoretical work (Polyakov and Mineev, 2000; Schauble et al., 2001; Schauble, 2004) and later proposed by Williams et al. (2005). On the other hand, isotope fractionation of the magnitude indicated by trend B would produce isotopically heavy melts with δ^{56}Fe of ≈0.25–0.3, i.e. significantly heavier than average basalts. Indeed, Fe isotope compositions of basalts and peridotites (Fig. 1) indicate a more limited isotope fractionation, on the order of $\Delta^{56}Fe_{\text{mantle-melt}} \approx 0.1$ Weyer et al., 2005; Schoenberg and von Blanckenburg, 2006; Weyer et al., in press, this study) and more consistent with trend A (which includes all analysed peridotites).

Several alternative interpretations can be put forward to explain the two trends.

(1) Trend B is produced not by partial melting, but by a metasomatic process that had the same effect for all three localities. In such a case, using trend B would lead to an overestimation of isotopic fractionation during partial melting. However, the absence of evidence for significant metasomatic enrichments in these samples argues against this hypothesis.
(2) The slope of trend B was modified by diffusion or disequilibrium dissolution of mantle minerals with preferential transport of Fe from the solid to the melt, resulting in high Mg#. However, during a kinetic process light Fe isotopes should preferentially enter the melt because they diffuse faster than heavy Fe isotopes (Richter et al., 2003). This should result in a positive, rather than the observed negative, correlation of δ^{56}Fe and Mg#.
(3) Alternatively, trend B is produced by partial melting, and many of the additional samples from other localities used for trend A were affected by metasomatic processes after partial melting which modified their Fe isotope composition.

In fact, the very low correlation coefficient of trend A ($R^2 = 0.3$) indicates that the samples were affected by several processes. Thus, the similarity of the fractionation

factor implied by trend A to that obtained with the average mantle–basalt approach might be coincidental. Notably, most depleted samples from other localities, which do not match the $1000\ln\alpha = 0.3$ per mil trend, plot above this line towards heavier Fe isotope compositions. This may be due to isotopic re-equilibration of the ascending melt with the depleted, and thus isotopically lighter, residual lithospheric mantle. Such a phenomenon would produce variable, but on average heavier, isotope compositions in mantle peridotites affected by these processes. At the same time, the peridotite–melt exchange would produce lighter isotope compositions in the melts.

Our results do not furnish direct evidence for the above hypothesis. We note, however, that all four spinel lherzolites from Horoman in this study plot on trend B whereas two plagioclase lherzolites from Horoman plot off that trend (Fig. 3b). The plagioclase lherzolites have distinctly higher contents of all trace elements relative to spinel lherzolites (Takazawa et al., 2001). This can be interpreted as a reaction of the originally depleted mantle rocks with a large amount of an MORB-like melt. Such a significant metasomatic overprint would have an effect on Fe isotope composition of the peridotites as well. Generally, reaction and equilibration of depleted peridotites (that have light Fe isotope signatures) with melts (that are enriched in heavy Fe isotopes) will produce a more heterogeneous lithospheric mantle and diminish the difference in Fe isotope compositions between the average lithospheric mantle and the basalts.

Finally, mantle dynamics will cause continuous recycling of both depleted and enriched lithosphere into source regions of partial melting. For that reason, partial melting trends of individual peridotite series may not match each other completely. Nevertheless, the partial melting trends for three individual peridotite series, which together make up trend B, overlap very tightly (Fig. 2b). Trend B was modelled here with an initial value for $\delta^{56}Fe = 0.05$ at $Mg\#_{PM} = 0.894$ (Mg# of the primitive mantle McDonough and Sun, 1995). This initial best agrees with the linear regression line for these localities (Fig. 2b). However, a better estimate of the average Fe isotope composition of the entire upper mantle is probably attained by using trend A, which includes a larger variety of mantle rocks from different localities (Fig. 2a). Interpolating this trend to $Mg\#_{PM}$ gives $\delta^{56}Fe \approx 0.02 \pm 0.03$. This value is in good agreement with the estimate of Weyer et al. (2005), which was based on a smaller amount of samples, as well as with the value of Weyer et al. (in press), which was based on a compilation of existing Fe isotope data for peridotites and basalts from the literature.

5.2. Metasomatic enrichment during melt percolation

Metasomatised peridotites from Tok and Tariat have highly variable Fe isotope compositions, which extend either towards increasingly heavy or to extremely light values with increasing enrichments in iron. Two different types of metasomatic enrichment can be distinguished.

E1-type metasomatism (Table 1, Tok samples 2-3, 2-10, 3-2, 3-22, 8-10, 10-2) is caused by reaction of residual peridotites with silica-undersaturated, Fe-rich melts leading to replacement of opx by cpx and the formation of wehrlites (Ionov et al., 2005a). This type of metasomatism leads to an increase in $\delta^{56}Fe$, resulting in correlations of Fe isotope compositions with cpx abundances, CaO and FeO contents and Mg# (Table 1, Fig. 2a–d). Because melts produced by partial melting have heavier Fe isotope compositions than mantle residues, the heavy Fe isotope signature might have been inherited form parental liquids that formed by partial melting of fertile mantle. However, a simple one-stage partial melting origin is not consistent with the inferred low Mg# and high Fe contents of the melts responsible for the E1-type metasomatism (Ionov et al., 2005a). Such melts must have underwent fractionation crystallisation and melt–rock reaction in mantle magma chambers and veins as indicated by common olivine-cpx cumulates and composite (veined) samples among the Tok xenoliths (Ionov et al., 2005a). The FeO enrichments and low Mg# of the LW series Tok peridotites were earlier reproduced by Ionov et al. (2005a) using a melt percolation model, in which an evolved silicate liquid with Mg# = 0.63 infiltrates a depleted peridotite with Mg# = 0.91. The low Mg# in the LW series rocks is explained in their model by high melt/rock ratios (between 0.5 and 5). Reaction of host residual peridotites with evolved silicate melts (Ionov et al., 2005a) is also consistent with the correlation of Fe isotopes with Zr and other incompatible trace elements (Fig. 2e + f).

Here, we assume (Fig. 4) that no Fe isotope fractionation occurs in the reaction: $melt_0 + opx = melt_f + cpx + olivine$. In this case, Fe isotope composition of the enriched peridotite (reaction product) can be simply calculated as isotopic equilibration of the Fe contained in the original depleted peridotite with the total Fe contained in the melt that reacted with the peridotite. For the depleted mantle we assume $\delta^{56}Fe = -0.042$ (from our model depletion trend in Fig. 3b at Mg# = 0.91) and for the melt we assume $\delta^{56}Fe = 0.3$ (assuming $\ln\alpha_{mantle\text{-}melt} \approx 0.3‰$ as indicated from Fig. 3b). The E1-type enriched peridotites are consistent with such a model, except for two wehrlites (10-1 and 10-3), which have slightly lighter Fe

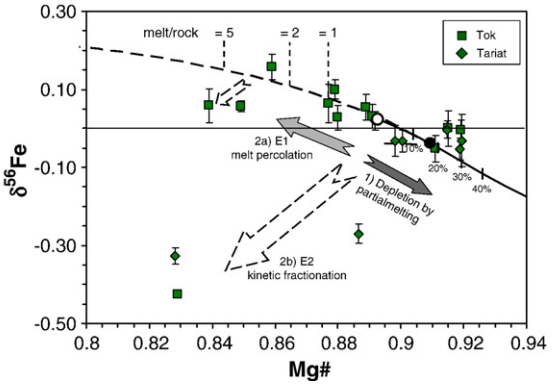

Fig. 4. Plot of δ^{56}Fe versus Mg# for mantle rocks from Tok and Tariat showing the depletion and enrichment history for these rocks. (1) The samples have been variably depleted by partial melting. (2) An enrichment event including: (a) infiltration of an isotopically heavy Fe-rich melt (E1) or (b) probably diffusion during melt percolation, resulting in isotopically light peridotites (E2). Depletion was modelled using a batch melting model with $\ln\alpha = 0.3‰$ (tick marks indicate degrees of melt extraction). For enrichment E1 the melt percolation model of Ionov et al. (2005a) was used (depleted peridotite: Mg# = 0.91, δ^{56}Fe = −0.042; melt: Mg# = 0.63, δ^{56}Fe = 0.3), assuming no isotope fractionation during melt–mineral reactions (see text for further explanation). Block arrows schematically indicate directions of various processes.

isotope compositions (Fig. 4). These two samples might have been additionally affected by E2-type metasomatism.

This second type of metasomatism (E2) produces very light Fe isotope compositions (Table 1; Tok sample 10-11, Tariat samples Z-9, Hr-25) combined with enrichment in the Fe content (Fig. 2c). Thus the trend of E2-type metasomatism in a plot of δ^{56}Fe versus Mg# is ± vertical to the trend defined by partial melting and E1-type metasomatism (Figs. 2d, 4). The E2-type peridotites have no (or only minor) enrichments in CaO or secondary cpx (Fig. 2a, b). In this case, no significant peridotite–melt phase reaction took place, and the Fe isotope effects were likely produced through chemical and isotopic exchange between the wall–rock mantle and the percolating melt (Ionov et al., 2005a, 2006a). This type of enrichment produced much lighter Fe isotope compositions than those usually observed in partial melting residues (Table 1, Fig. 3a and b). As already discussed by Williams et al. (2005) using mass balance considerations, recycled crustal components or subduction related hydrothermal fluids are unlikely to yield extremely light Fe isotope signatures in the mantle.

However, large isotope fractionations may be produced by the interaction of common mantle-derived liquids (as in the melt percolation model above) with the mantle by means of kinetic fractionation such as that induced by diffusion. Richter et al. (2003) observed Fe isotope fractionation of several per mil in diffusion experiments between a basaltic and a rhyolitic melt. Isotope fractionation during diffusion occurs because lighter isotopes generally diffuse faster than heavier isotopes (Richter et al., 2003). Thus, diffusion of Fe from an Fe-rich melt to a host peridotite in the course of E2-type metasomatism would explain both high Fe contents (low Mg#) and the light Fe isotope compositions without any modal changes in the peridotite. Alternatively, a disequilibrium reaction between the melt and the host peridotite accompanied by kinetic fractionation could also produce combined Fe and light Fe isotope enrichment, although there is no petrological evidence for such reactions in the Tok or Tariat peridotites. Such a reaction would result in a faster exchange of Fe between melt and host peridotite compared to diffusion (Williams et al., 2005).

Diffusion-induced metasomatic overprint on peridotites from Tok resulting in lithium elemental and isotopic disequilibria between the mineral phases was recently reported by Rudnick and Ionov (2007). Those authors inferred that Li diffusion in the Tok xenoliths stemmed from a hypothetical metasomatic event shortly preceding their entrainment into the host basalt. However, Fe diffusion is about two orders of magnitude slower than Li diffusion (Richter et al., 2003), and minerals of the Tok samples have practically identical (i.e. equilibrated) Fe isotope compositions (Table 1). Furthermore, only the rare E2-type samples from Tok have the light Fe isotope signatures while all Tok peridotites appear to have been affected by the late-stage Li diffusion (Rudnick and Ionov, 2007). This may also be valid for the E2-type Tariat mantle, even though no Li isotope measurements are available for these samples. This implies that interaction of the Tok mantle with the late-stage, Li-rich metasomatic fluids was not long enough to also affect the Fe isotope compositions of the peridotite minerals. By contrast, diffusion-driven melt metasomatism must have selectively affected the E2-type enriched peridotites. Given the lower diffusion rate for Fe compared to Li (Richter et al., 2003; Dohmen and Chakraborty, in press) and the equilibrated Fe isotope compositions of minerals in the E2-type peridotites (sample 10-11), the Fe-enrichment event at Tok inferred in this study probably occurred long before (>1 Ma) the Li-enrichment event proposed by Rudnick and Ionov and subsequent entrainment of the xenoliths into the host basalt, such that the minerals had enough time to re-equilibrate Fe isotopes.

Fractionation of Fe isotopes in E2-type peridotites could be further enhanced by chromatographic processes. Such processes can be compared with Fe isotope fractionation on ion exchange columns (Anbar et al., 2000). Within a mantle column, diffusion or a disequilibrium

reaction rather than adsorption onto the stationary phase might be the process leading to Fe isotope fractionation. Chromatographic fractionation models have been frequently applied to explain decoupling between trace elements or between Sr and Nd isotopes recorded in mantle peridotites (e.g. Navon and Stolper, 1987; Bodinier et al., 1990; Ionov et al., 2002; Bodinier et al., 2004; Ionov et al., 2005a, 2006b).

Though E1- and E2-types of metasomatism have different petrological, geochemical and Fe isotope signatures, they might have been produced within the same enrichment event but at different time and different locations. In the beginning, and close to the source, the percolating melt was probably silicate-undersaturated and CaO-rich (Ionov et al., 2005a), and thus reacted with opx and spinel to form wehrlites (olivine + cpx) that are enriched both in Fe and in heavy Fe isotopes. After continuous migration of the melt through the mantle column, further away from the source, its chemical composition likely changed from silica-undersaturated to silica-saturated through continuous reaction with host opx-bearing peridotites. Such a melt will not react with opx anymore. Instead, diffusion might be the dominant melt–peridotite exchange process responsible for the E2-type metasomatism.

5.3. Fe isotope composition of basalts

Several processes can be taken into account to explain the Fe isotopic features of the basalts. As explained above, partial melting is the most likely process to explain the heavier Fe isotope composition of average basalts (≈0.1‰) compared to peridotites. If Fe isotope fractionation during partial melting is as high as inferred from trend B, even heavier Fe isotope compositions should be expected for basalts. However, re-equilibration of "heavy" melts with "light" depleted peridotites may reduce the difference in Fe isotope composition between the basalts erupted on the surface and the mantle residues. Additionally, metasomatic processes, such as melt percolation, might cause Fe isotope variations in basalts generated from such mantle source, although pooling of melts in deep magma chambers (e.g. for MORB) will limit the scope of such variations.

In theory, basalts should become heavier during fractional crystallisation because fractionation factors between the basaltic melt and minerals (olivine, cpx) crystallizing from the melt can be expected to be similar to those during partial melting (i.e. between basalts and the mantle residue). This is also indicated by results of Poitrasson et al. (2004), who reported a significantly lighter Fe isotope composition of olivine phenocrysts from a lunar sample (12045.13) compared to their host magma. Likewise, Poitrasson and Freydier (2005) obtained heavy Fe isotope compositions for highly evolved granites, which may imply Fe isotope fractionation during magma differentiation.

In this study, however, we do not observe a correlation between δ^{56}Fe and Mg#, as an index of differentiation degrees, for basalts. Probably, heterogeneities in δ^{56}Fe inherited from the source and those caused by interactions of the magma with wall–rocks overwhelmed the effect of fractional crystallisation. Such effects might be distinguished in a suite of basalts and differentiates originated from the same source, which is beyond the scope of this study.

We note, however, that the OIBs in our study tend towards slightly heavier Fe isotope compositions than MORBs, even though the average values for OIBs and MORBs cannot be distinguished at 95% coincidence level. In our model, the heavier Fe isotope compositions of OIBs could be explained either by their relatively low melting degrees (resulting in greater fractionation during partial melting) or by usually higher degrees of fractional crystallisation (which should result in additional Fe isotope fractionation). Moreover, OIBs originate from deeper mantle levels and are typically transported more rapidly to the surface than MORB (that is why some OIBs carry mantle xenoliths). Thus, their degrees of re-equilibration with the depleted, isotopically light, lithospheric mantle must be generally lower.

6. Conclusions

Iron isotope compositions can provide new insights into mantle processes, such as partial melting and metasomatism. The processes that might affect Fe isotope compositions of peridotites and mantle-derived rocks, based on observations of this study, are schematically summarized in Fig. 5. Our new data on mantle rocks from several petrologically well-studied localities (Horoman, Kamchatka, Lherz) display trends of Fe isotope compositions versus modal or chemical indices of partial melting (such as Mg#) indicating that Fe isotopes fractionate during melt extraction from the mantle. Fe isotope fractionation on the order of 0.1‰ during partial melting was earlier predicted based on average Fe isotope compositions of mantle peridotites and basalts (Weyer et al., 2005, in press). However, the least disturbed partial melting trends established in this study imply a significantly higher fractionation factor for Fe isotopes between melt and mantle residue on the order of $\ln\alpha = 0.3$‰. Two alternatives can be proposed to explain those findings. (1) Disequilibrium peridotite–

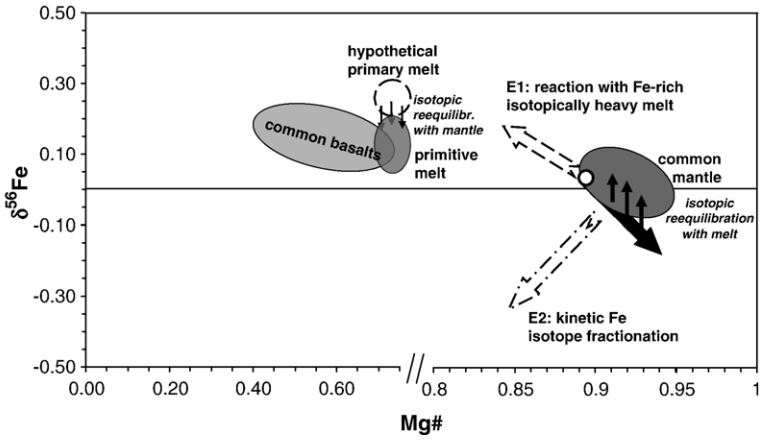

Fig. 5. Sketch of all processes described in this study, which influence Fe isotope compositions of mantle rocks and basalts. During partial melting, an isotopically light mantle residue (black block arrow) and an isotopically heavy primary melts (dashed field) are produced. Isotopic re-equilibration during melt ascent probably reduces the Fe isotope fractionation between mantle and basalts (grey ecliptic fields, labelled as common mantle and primitive basalts). In theory, differentiation of basalts should lead to a further increase in δ^{56}Fe of basalts bringing them to the field labelled here as common basalts (correlation of Mg# and δ^{56}Fe was not observed in this study). Metasomatic enrichment processes, such as melt infiltration and kinetic Fe isotope fractionation (likely diffusion) during melt percolation, can lead to heavy or extremely light Fe isotope compositions, respectively (indicated by dashed block arrows).

melt reactions may cause particularly strong Fe isotope fractionation (with $\ln\alpha \approx 0.3‰$) for the samples of trend B, though kinetic fractionation during diffusion of Fe from mantle minerals into the melt should preferentially enrich the light Fe isotopes in the melt. (2) Re-equilibration of the isotopically heavy primary melt with the depleted isotopically light lithospheric mantle results in reduced isotopic differences between mantle and basalts. This and other metasomatic processes could be superimposed on the general depletion trend of peridotites from various localities (trend A) and reduce its slope. This latter trend of all the mantle samples analysed in this study was used to estimate the average Fe isotope composition of the upper mantle (Figs. 1, 3a) to yield $\delta^{56}Fe \approx 0.02 \pm 0.03$. Assuming that the upper mantle has the same Fe isotope composition as the bulk Earth (the major uncertainty of this assumption lies probably in the poorly defined Fe isotope composition of the core (e.g. Weyer et al., 2005; Poitrasson et al., 2005) this implies that Fe isotope compositions of the Earth and the solar system (i.e. chondrites) are identical within uncertainties (Weyer et al., in press and references therein).

The effects of interaction between mantle melts and residues on δ^{56}Fe are particularly large if Fe-rich (low-Mg#) melts are involved. This is evident for several metasomatised peridotites from Tok (Siberia) and Tariat (Mongolia). For these localities, Fe isotopes can help to distinguish two types of melt metasomatism. One of them (E1) is characterized by the formation of abundant secondary cpx through peridotite–melt reaction and results in heavier than average mantle Fe isotope compositions. In contrast, Fe-enrichment through peridotite–melt exchange without significant modal changes (E2) results in extremely light Fe isotope compositions (up to $\delta^{56}Fe = -0.42$). The most likely process to explain such light Fe isotope compositions at mantle temperatures (as observed for E2-type peridotites) is diffusion of Fe from an Fe-rich melt into the depleted peridotites. Chromatographic effects that accompany the percolation of melt through mantle peridotites could further enhance the isotopic variation between the E1 and E2-type metasomatised peridotites. The result of such a process would be to produce isotopically very light Fe isotope compositions in the percolation columns assuming continuous Fe diffusion from the Fe-rich melt to the mantle residue. In contrast, reaction of such an isotopically heavy melt with the host mantle would produce heavy Fe isotope compositions assuming high time-integrated melt/rock ratios. Thus, one and the same metasomatic process probably produced different metasomatic effects in terms of Fe isotope compositions similarly to the effects observed in terms of major and trace element fractionation and Sr–Nd isotope decoupling (Bodinier et al., 1990; Ionov et al., 2002; Bodinier et al., 2004; Ionov et al., 2006b).

Acknowledgements

We are grateful to Alan Woodland and Eiichi Takazawa for providing peridotite samples (Lherz and Horoman, respectively) and to Karsten Haase for providing 10 fresh basalt glasses. We thank Gerhard Brey, Alan Woodland and Ariel Anbar for fruitful discussions.

Anna Neumann and Eugenia Gromov are thanked for laboratory assistance. Helen Williams and an anonymous reviewer are thanked for their constructive reviews which helped to improve the discussion. We thank Sumit Chakraborty for providing unpublished diffusion data for Fe in olivine. Dmitri Ionov acknowledges a Mercator guest professorship from the German Research Society (DFG) at Goethe-Universität, Frankfurt am Main in 2005–2006.

Appendix A. Supplementary data

Supplementary data associated with this article can be found, in the online version, at doi:10.1016/j.epsl.2007.04.033.

References

Anbar, A.D., Roe, J.E., Barling, J., Nealson, K.H., 2000. Nonbiological fractionation of iron isotopes. Science 288, 126–128.

Arnold, G.L., Weyer, S., Anbar, A.D., 2004. Fe isotope variation in natural materials measured using high mass resolution MC-ICPMS. Anal. Chem. 76, 322–327.

Beard, B.L., Johnson, C.M., 2004. Inter-mineral Fe isotope variations in mantle-derived rocks and implications for the Fe geochemical cycle. Geochim. Cosmochim. Acta 68, 4727–4743.

Bodinier, J.L., Vasseur, G., Verniers, J., Dupuy, C., Fabries, J., 1990. Mechanism of mantle metasomatism: geochemical evidence from the Lherz Orogenic Peridotite. J. Petrol. 31, 597–628.

Bodinier, J.-L., Menzies, M.A., Shimuzu, N., Frey, F.A., McPherson, E., 2004. Silicate, hydrous and carbonate metasomatism at Lherz, France: contemporaneous derivatives of silicate melt–harzburgite reaction. J. Petrol. 45, 299–320.

Dohmen, R., Chakraborty, S., (in press). Fe–Mg diffusion in olivine II: point defect chemistry, change of diffusion mechanisms and a model for calculation of coefficients in natural olivine. Phys. Chem. Miner.

Elliott, T., Thomas, A., Jeffcoate, A., Niu, Y., 2006. Lithium isotope evidence for subduction-enriched mantle in the source of mid-ocean-ridge basalts. Nature 443, 565–568.

Fretzdorff, S., Haase, K.M., 2002. Geochemistry and petrology of lavas from the submarine flanks of Reunion Island (Western Indian Ocean): implications for magma genesis and the mantle source. Mineral. Petrol. 75, 153–184.

Haase, K.M., 2002. Geochemical constraints on magma sources and mixing processes in Easter Microplate MORB (SE Pacific): a case study of plume–ridge interaction. Chem. Geol. 182, 335–355.

Herzberg, C., 2004. Geodynamic information in peridotite petrology. J. Petrol. 45, 2507–2530.

Hofmann, A.W., 2004. Sampling mantle heterogeneity through oceanic basalts: isotopes and trace elements. In: Carlson, R. (Ed.), The Mantle and the Core. . Treatise on Geochemistry, vol. 2. Elsevier Pergamon, pp. 61–101.

Ionov, D.A., Compositional variations and heterogeneity in fertile lithospheric mantle: peridotite xenoliths in basalts from Tariat, Mongolia, Contributions to Mineralogy and Petrology (in press).

Ionov, D.A., Hofmann, A.W., 2006. Depth of formation of sub-continental peridotites. Earth Plant. Sci. Lett. (submitted for publication).

Ionov, D.A., Hofmann, A.W., Shimuzu, N., 1994. Metasomatism-induced melting in mantle xenoliths from Mongolia. J. Petrol. 35, 753–785.

Ionov, D.A., O'Reilly, S.Y., Griffin, W.L., 1998. A geotherm and lithospheric section for Central Mongolia (Tariat Region). In: Flower, M.F.J., et al. (Eds.), Mantle Dynamics and Plate Interactions in East Asia. Amer. Geophys. Union.

Ionov, D.A., Bodinier, J.-L., Mukasa, S.B., Zanetti, A., 2002. Mechanisms and sources of mantle metasomatism: major and trace element compositions of Peridotite xenoliths from Spitzbergen in the context of numerical modelling. J. Petrol. 43, 2219–2259.

Ionov, D.A., Chanefo, I., Bodinier, J.-L., 2005a. Origin of Fe-rich lherzolites and wehrlites from Tok, SE Siberia by reactive melt percolation in refractory mantle peridotites. Contributions to Mineralogy and Petrology 150, 335–353.

Ionov, D.A., Prikhodko, V.S., Bodenier, J.-L., Sobolov, A.V., Weis, D., 2005b. Lithospheric mantle beneath the south-eastern Siberian craton: petrology of peridotite xenoliths in basalts from the Tokinsky Stanovik. Contributions to Mineralogy and Petrology 149, 647–665.

Ionov, D.A., Chazot, G., Chauvel, C., Merlet, C., Bodinier, J.-L., 2006a. Trace element distribution in peridotite xenoliths from Tok, SE Siberian craton: a record of pervasive, multi-stage metasomatism in shallow refractory mantle. Geochimica et Cosmochimica Acta 70, 1231–1260.

Ionov, D.A., Shirley, S.B., Weis, D., Brügmann, G., 2006b. Os–Hf–Sr–Nd isotope and PGE systematics of spinel peridotite xenoliths from Tok, SE Siberian craton: effects of pervasive metasomatism in shallow refractory mantle. Earth Planet. Sci. Lett. 241, 47–64.

Kinzler, R.J., 1997. Melting of mantle peridotite at pressures approaching the spinel to garnet transition: application to mid-ocean ridge basalt petrogenesis. J. Geophys. Res. -Solid Earth 102, 853–874.

Langmuir, C.H., Klein, E.M., Plank, T., 1992. Petrology systematics of mid-ocean ridge basalts: constraints on melt generation beneath ocean ridges. In: Morgan, P., Blackman, D.K., Sinton, J.M. (Eds.), Mantle Flow and Melt Generation at Mid-Ocean Ridges. Geophysical Monograph, vol. 71. American Geophysical Union, pp. 183–280.

McDonough, W.F., Sun, S.-S., 1995. The composition of the Earth. Chem. Geol. 120, 223–253.

Navon, O., Stolper, E., 1987. Geochemical consequences of melt percolation: the upper mantle as a chromatographic column. J. Geol. 95, 285–307.

Poitrasson, F., Freydier, R., 2005. Heavy iron isotope composition of granites determined by high resolution MC-ICP-MS. Chem. Geol. 222, 132–147.

Poitrasson, F., Halliday, A., Lee, D., Levasseur, S., Teutsch, N., 2004. Iron isotope differences between Earth, Moon, Mars and Vesta as possible records of contrasted accretion mechanisms. Earth Planet. Sci. Lett. 223, 253–266.

Poitrasson, F., Levasseur, S., Teutsch, N., 2005. Significance of iron isotope mineral fractionation in pallasites and iron meteorites for the core–mantle differentiation of terrestrial planets. Earth Planet. Sci. Lett. 234, 151–164.

Polyakov, V.B., Mineev, S.D., 2000. The use of Mössbauer spectroscopy in stable isotope geochemistry. Geochimica et Cosmochimica Acta 64, 849–865.

Press, S., Witt, G., Seck, H.A., Inov, D., Kovalenko, V.I., 1986. Spinel peridotite xenoliths from the Tariat depression, Mongolia. I: Major element chemistry and mineralogy of a primitive mantle xenolith suite. Geochim. Cosmochim. Acta 50, 2587–2599.

Richter, F.M., Davis, A.M., DePaolo, D.J., Watson, E.B., 2003. Isotope fractionation by chemical diffusion between molten basalt and rhyolite. Geochim. Cosmochim. Acta 67, 3823–3905.

Rudnick, R.L., Ionov, D.A., 2007. Lithium elemental and isotopic disequilibrium in minerals from peridotite xenoliths from far-east Russia: product of recent melt/fluid–rock reaction. Earth Planet. Sci. Lett. 256, 278–293.

Russel, W.A., Papanastassiou, D.A., Tombrello, T.A., 1978. Ca isotope fractionation on the Earth and other solar system materials. Geochim. Cosmochim. Acta 42, 1075–1090.

Schauble, E.A., 2004. Applying stable isotope fractionation theory to new systems. In: Johnsos, C.M., Beard, B.L., Albarede, F. (Eds.), Geochemistry of Non-traditional Stable Isotopes. Rewiews in Mineralogy and Geochemistry, vol. 55, pp. 65–111.

Schauble, E.A., Rossman, G.R., Taylor, H.P., 2001. Theoretical estimates of equillibrium Fe-isotope fractionation from vibrational spectroscopy. Geochim. Cosmochim. Acta 65, 2487–2497.

Schoenberg, R., von Blanckenburg, F., 2006. Modes of planetary-scale Fe isotope fractionation. Earth Planet. Sci. Lett. 252, 342–359.

Schoenberg, R., von Blankenburg, F., 2005. An assessment of the accuracy of stable Fe isotope ratio measurements on samples with organic and inorganic matrices by high resolution multicollector ICP-MS. Int. J. Mass Spectrom. 242, 257–272.

Seitz, H.-M., Brey, G., Lahaye, Y., Durali, S., Weyer, S., 2004. Lithium isotopic signatures of peridotite xenoliths and isotopic fractionation at high temperature between olivine and pyroxenes. Chem. Geol. 212, 163–177.

Takazawa, E., Frey, F.A., Shimuzu, N., Obata, M., 2000. Whole rock compositional variations in an upper mantle peridotite (Horoman, Hokkaido, Japan): are they consistent with a partial melting process? Geochim. Cosmochim. Acta 64, 695–716.

Walter, M.J., 1998. Melting of garnet peridotite and the origin of komatiite and depleted lithosphere. J. Petrol. 39, 29–60.

Weyer, S., Schwieters, J.B., 2003. High precision Fe isotope measurements with high mass resolution MC-ICPMS. Int. J. Mass Spectrom. 226, 355–368.

Weyer, S., Münker, C., Mezger, K., 2003. Nb/Ta, Zr/Hf and REE in the depleted mantle: implications for the differentiation history of the crust–mantle system. Earth Planet. Sci. Lett. 205, 309–324.

Weyer, S., Woodland, A., Münker, C., Arnold, G., Chakrabarti, R., Anbar, A., 2004. Iron isotope variations in the Earth's mantle and the terrestrial planets. Geochimica et Cosmochimica Acta 68, A1113.

Weyer, S., Anbar, A.D., Brey, G.P., Münker, C., Mezger, K., Woodland, A.B., 2005. Iron isotope fractionation during planetary differentiation. Earth Planet. Sci. Lett. 240, 251–264.

Weyer, S., Anbar, A.D., Brey, G.P., Müncker, C., Mezger, K., Woodland, A.B., 2007. Fe-isotope fractionation during partial melting on Earth and the current view on the Fe-isotope budgets of the planets (reply to the comment of F. Poitrasson and to the comment of B.L. Bead and C.M. Johnson on "Iron isotope fractionation during planetary differentiation" by S. Weyer, A.D. Anbar, G.P. Brey, C. Münker, K. Mezger and A.B. Woodland). Earth Planet. Sci. Lett. 256, 638–646.

Williams, H., McCammon, C., Peslier, A., Halliday, A., Teutsch, N., Levasseur, S., Burg, J., 2004. Iron isotope fractionation and the oxygen fugacity of the mantle. Science 304, 1656–1659.

Williams, H., Peslier, A., McCammon, C., Halliday, A., Levasseur, S., Teutsch, N., Burg, J., 2005. Systematic iron isotope variations in mantle rocks and minerals: the effect of partial melting and oxygen fugacity. Earth Planet. Sci. Lett. 235, 435–452.

Woodland, A.B., Kornprobst, J., Wood, B.J., 1992. Oxygen thermobarometry of orogenic lherzolite massifs. J. Petrol. 33, 203–230.

Woodland, A.B., Kornprobst, J., McPherson, E., Bodenier, J.-L., Menzies, M.A., 1996. Metasomatic interactions in the lithospheric mantle: petrologic evidence from the Lherz massif, French Pyrenees. Chem. Geol. 134, 83–112.

Zhu, X.-K., Guo, Y., O'Nions, R.K., Young, E.D., Ash, H.D., 2001. Isotopic heterogeinity of iron in the early solar system. Nature 412, 311–313.

Zhu, X.K., Guo, Y., Williams, R.J.P., O'Nions, R.K., Matthewsa, A., Belshaw, N.S., Canters, G.W., de Waal, E.C., Weser, U., Burgess, B.K., Salvato, B., 2002. Mass fractionation processes of transition metal isotopes. Earth and Planetary Science Letters 220, 47–62.